Uluslararası İleri Doğa Bilimleri ve Mühendislik Araştırmaları Dergisi
Sayı 8, S. 16-24, 8, 2024

Araştırma Makalesi

IJANSER

International Journal of Advanced Natural Sciences and Engineering Researches
Volume 8, pp. 16-24, 8, 2024

Research Article

https://as-proceeding.com/index.php/ijanser
ISSN: 2980-0811

Activation of Red Mud and its Application to FRP-Confined Geopolymer Concrete

Shahir Ahmad Safi[*1], Khaled Waleed Radman [1], and Ali Raza [1]

[1]*Department of Civil Engineering, University of Engineering and Technology Taxila, 47050, Pakistan*

[*]*(shahirahmad229@gmail.com)*

(Received: 03 September 2024, Accepted: 18 September 2024)

(3rd International Conference on Scientific and Innovative Studies ICSIS 2024, September 11-12, 2024)

ATIF/REFERENCE: Safi, S. A., Radman, K. W. & Raza, A. (2024). Activation of Red Mud and its Application to FRP-Confined Geopolymer Concrete. *International Journal of Advanced Natural Sciences and Engineering Researches*, 8(8), 16-24.

Abstract – As sustainability gains importance, the demand for low-carbon materials is rising. Geopolymer concrete (GC), using waste materials, is a promising eco-friendly alternative to traditional concrete but has relatively low long-term compressive strength. This study investigates the impact of carbon fiber reinforced polymer (CFRP) confinement on the axial performance of activated red mud-based geopolymer concrete (RMGC). Testing 36 cylindrical RMGC samples with strengths of 15 MPa and 30 MPa, and one or two layers of CFRP sheets, revealed significant strength improvements. For 15 MPa RMGC, CFRP layers increased compressive strength by up to 153.85%, and for 30 MPa RMGC, up to 99.33%. CFRP confinement was more effective in enhancing the properties of lower-strength RMGC.

Keywords – Activated Red Mud, CFRP Sheets, Geopolymer Concrete, Compressive Strength, Stress-Strain Curves.

I. INTRODUCTION

Geopolymer (GP) materials are increasingly recognized for their sustainability advantages over traditional cement-based concrete, primarily due to their lower carbon emissions. As a result, they are becoming more prominent in engineering applications, especially in structural engineering. GP composites offer significant flexibility in incorporating various industrial and non-industrial by-products and wastes [1, 2]. Despite this, the effects of these waste materials on GP composites are not yet fully understood. Red mud, a by-product from alumina production, currently amounts to 5 billion tons globally. This waste contributes to over 60% of China's emissions, with its stockpile increasing by 120 million tons annually [3]. The high alkalinity of red mud limits its usage, and its open-air storage has detrimental environmental impacts [4]. Red mud primarily contains goethite, feldspar, calcite, and some amorphous aluminosilicate, which offer limited cementing potential [5].

In addressing challenges related to structural integrity, engineers are increasingly focusing on fiber-reinforced polymers (FRP). FRPs are effective for repairing under-reinforced columns and enhancing their load-bearing capacity. Concrete structures exposed to harsh conditions often face significant durability issues, and FRP systems are commonly employed to reinforce and repair these structures, potentially extending their lifespan. FRPs offer several advantages, including ease of application, enhanced durability, increased strength, and greater stiffness. The effectiveness of FRP confinement is significantly influenced

by the geometry and shape of structural components. For instance, circular cross-section columns are advantageous as they allow the FRP fibers to interact fully with the column's cross-section [7]. This method not only improves structural response but also enhances durability [8]. Carbon fiber-reinforced polymer (CFRP) has notably impacted the construction industry by providing benefits such as minimal disturbance and ease of handling [9].

To ensure the successful application of geopolymer concrete (GC) derived from waste materials in construction, it is essential to improve its structural performance. One effective method for achieving the desired structural properties is lateral confinement of GC. This study aims to evaluate the behavior of CFRP-confined geopolymer concrete, specifically using activated red mud (RMGC), under axial compression. The study involved applying various layers of CFRP sheets to laterally confine RMGC specimens and examined the effects of CFRP confinement on the unconfined strengths of RMGC samples, ranging from 15 MPa to 30 MPa. Additionally, the research explored how different numbers of CFRP laminates affected the stress-strain characteristics and failure patterns of the confined RMGC.

II. EXPERIMENTAL SETUP

i. Materials and Properties

In this study, Ground Granulated Blast Furnace Slag (GGBS) and calcined red mud were employed as binders to produce Reactive Magnesia Geopolymer Concrete (RMGC). Table 1 details the chemical compositions of GGBS and red mud, while Figure 1 illustrates the results of the sieve analysis. The average particle sizes of red mud and GGBS were found to be 36.5 µm and 9.5 µm, respectively, with surface areas of 0.39 m^2/g and 0.68 m^2/g. Activators used in the study included water glass and sodium hydroxide (NaOH). Recycled coarse aggregates (RCA), with a maximum particle size of 20 mm, were sourced from concrete cylinders less than a year old. The quartz sand particles used ranged from 435 to 610 µm. Initially, the red mud was ground for ten minutes, dried in a blast drying oven at 100 °C, and then processed in a testing mill for calcination preparation. The ground red mud was mixed with 10% water by weight to form testing cakes with a diameter of 20 cm and a thickness of 1-2 cm. These cakes were subsequently calcined in a muffle furnace according to a specified heating schedule, with calcination temperatures set at 500, 600, 700, and 800 degrees Celsius.

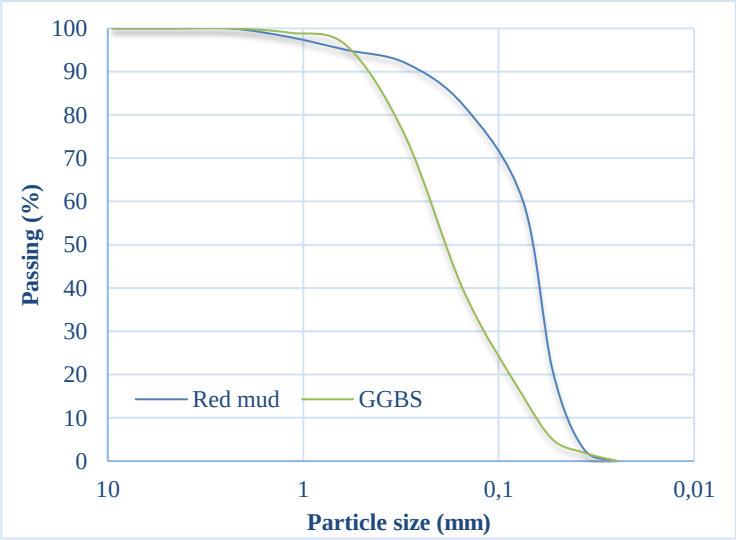

Figure 1. Sieve analysis of red mud and GGBS

Table 1. Chemical composition of red mud and GGBS.

Compound	Red mud (%)	GGBS (%)
Iron oxide (Fe_2O_3)	12.35	4.57
Alumina (Al_2O_3)	33.22	16.11
Calcium Oxide (CaO)	10.52	34.70
Silica (SiO_2)	24.56	32.22
Sodium oxide (Na_2O)	10.55	3.11
Magnesium Oxide (MgO)	3.05	1.77
Pottasium Oxide (K_2O)	3.11	3.26
Titania (TiO_2)	1.01	2.68
Lost on Ignition (LOI)	1.63	1.59

To prepare the mortar specimens, red mud and Portland cement were mixed in a 3:7 mass ratio. The effectiveness of the red mud was assessed by comparing the compressive strength of the mortar containing red mud with that of mortar made solely from Portland cement after 28 days. Red mud was subjected to calcination at temperatures of 500, 600, 700, and 800 degrees Celsius. The reactivity of the red mud at these temperatures was evaluated using an activity index. As shown in Figure 2, the activity index of red mud increased with higher calcination temperatures initially but then decreased. Specifically, the activity index rose to a maximum of 0.88 at 700°C before falling to 0.78 at 800°C, compared to the initial value of 0.66. This indicates that there is an optimal calcination temperature for red mud, beyond which its reactivity diminishes. This observation is consistent with previous research [1, 2], which noted that calcination temperatures of 500, 600, 700, and 800°C were investigated, with 800°C identified as optimal. The variations observed can be attributed to the original red mud's high calcite content.

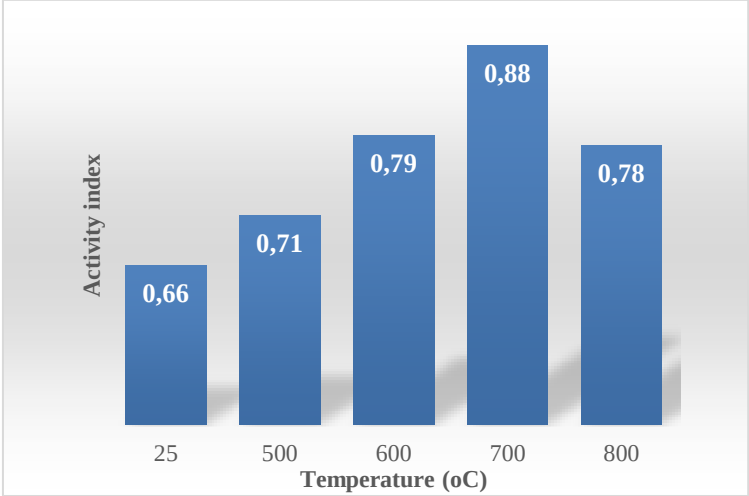

Figure 2. Activity indices of red mud at different temperatures

Red mud was initially ground for fifteen minutes and then sifted through a 75 µm square mesh. Its chemical makeup was analyzed using X-ray fluorescence (XRF), and thermal properties were investigated with a differential thermal analyzer (DTA). To determine the mineral content of both raw and calcined red mud at various temperatures, X-ray diffraction (XRD) was employed. Additionally, Fourier transform infrared spectroscopy (FTIR) was used to examine the molecular structure.

The thermogravimetric (TGA) and differential thermal analysis (DTA) curves for the unprocessed red mud are depicted in Figure 3. The TGA curve indicates a mass loss of 42.89% as the temperature increases from 0°C to 710°C. The majority of this mass loss occurs between 400°C and 700°C, primarily due to the release of both free and bound water during the pyrolysis phase from 0°C to 400°C. The DTA curve shows a significant exothermic peak in the 400–700°C range, likely due to the decomposition of

calcium carbonate, which forms from the carbonation of hydrated calcium silicate and typically decomposes between 500°C and 800°C. As the temperature rises, calcium carbonate in red mud decomposes into carbon dioxide and calcium oxide. This process is confined to a specific temperature range, with a notable weight reduction around 700°C, signifying an extremely reactive and unstable mineral structure. At approximately 700°C, the mineral composition of red mud stabilizes, as evidenced by the DTA curve, which shows no further endothermic or exothermic peaks. Therefore, the temperature range of 400°C to 700°C is critical for altering the mineral structure of red mud, while temperatures between 0°C and 400°C are mainly responsible for eliminating structural and free water.

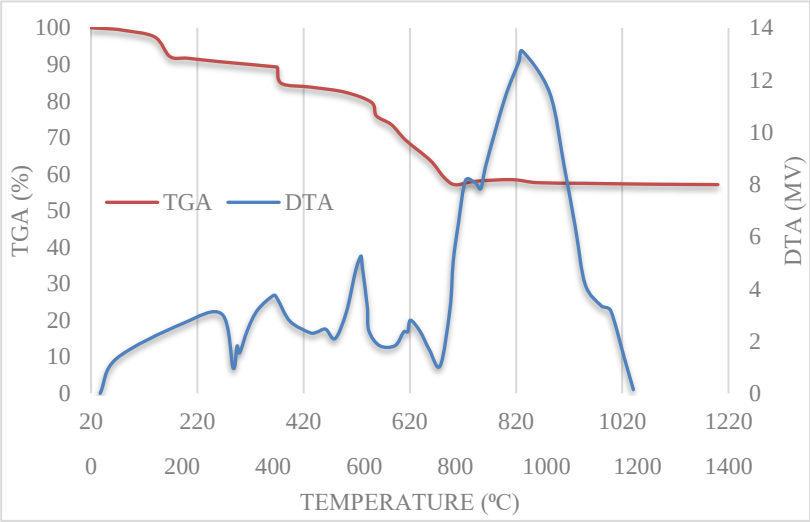

Figure 3. TGA—DTA curves of the original red mud.

In this study, CFRP sheets with a thickness of 0.12 mm were utilized. Laboratory tests assessed the tensile strength of these sheets, with the average findings presented in Table 2. Three CFRP sheets, each sized 130 mm in length and 20 mm in width, were tested for tensile properties. The tests were carried out at a loading rate of 0.033 mm/s, revealing that the CFRP sheets possess an elastic modulus of 35 GPa.

Table 2. Properties of CFRP sheets

Variables	Values	Variables	Values
Density	1.67 gm/m^2	Elastic modulus	35 GPa
Thickness	0.12 mm	Tensile strength	3450 MPa
Ultimate strain	1.69%	Fiber orientation	0º

ii. Manufacturing and Testing of Samples

A trial-and-error approach was employed to develop a mix of Reactive Magnesia Geopolymer Concrete (RMGC) with two specified compressive strengths, detailed in Table 3. Thirty-six cylindrical samples, each measuring 150 x 300 mm, were tested to assess the impact of Carbon Fiber Reinforced Polymer (CFRP) confinement on RMGC. These samples were divided into two main groups: one group consisted of 9 samples with a compressive strength of 15 MPa, and the other group had 9 samples with a strength of 30 MPa. To enhance the adhesion of the CFRP, the surfaces of the samples were prepared using grinding. CFRP sheets were then applied with resins boasting tensile strengths exceeding 85 MPa. Within each strength category, the specimens were further divided: six were left unreinforced (NL), six had double CFRP layers (DL), and six had a single CFRP layer (SL). Uniaxial compression tests were conducted on all RMGC samples, both with and without CFRP confinement, to generate stress-strain curves. This testing allowed for the evaluation of the improvements in ductility and strength due to CFRP confinement. The tests were conducted according to ASTM C39 standards, 28 days post-casting [4]. Compressive strength was measured in a displacement-controlled setup at a rate of 0.003 mm/s, as illustrated in Figure 4.

Figure 4. Testing of samples under axial compressive

Table 3. Ingredients of fabricated mixes.

Ingredients		Unit	15 MPa group	30 MPa group
Mineral admixtures	Red mud	Kg/m³	702	468
	GGBS	Kg/m³	78	312
Sand		Kg/m³	490	490
RCA		Kg/m³	785	785
Alkali activator (g)	Modulus	-	1.4	1.4
	Water glass	Kg/m³	471	471
	NaOH	Kg/m³	63.58	63.58
	Water	Kg/m³	94.75	94.75

III. RESULTS AND DISCUSSION

i. Failure Models

The load-bearing performance of SL and DL designs in FRP-confined specimens was markedly superior to that of unconfined samples, such as NL. As shown in Figure 5, specimens with FRP confinement exhibited sudden failures when reaching their peak tensile strength. During compressive testing, most RMGC specimens collapsed without producing noticeable debris. The incorporation of CFRP confinement significantly enhanced the concrete's ductility and strength. However, extreme loading conditions, such as axial splitting due to excessive compressive stress leading to radial cracks, radial expansion stresses causing CFRP rupture, concrete core crushing under high loads, CFRP sheet peeling due to poor bonding, and CFRP wrap buckling under axial loads, could still lead to failure. To ensure structural safety, it is crucial to understand these failure mechanisms, and establishing effective design guidelines necessitates both numerical modelling and experimental testing [5-8].

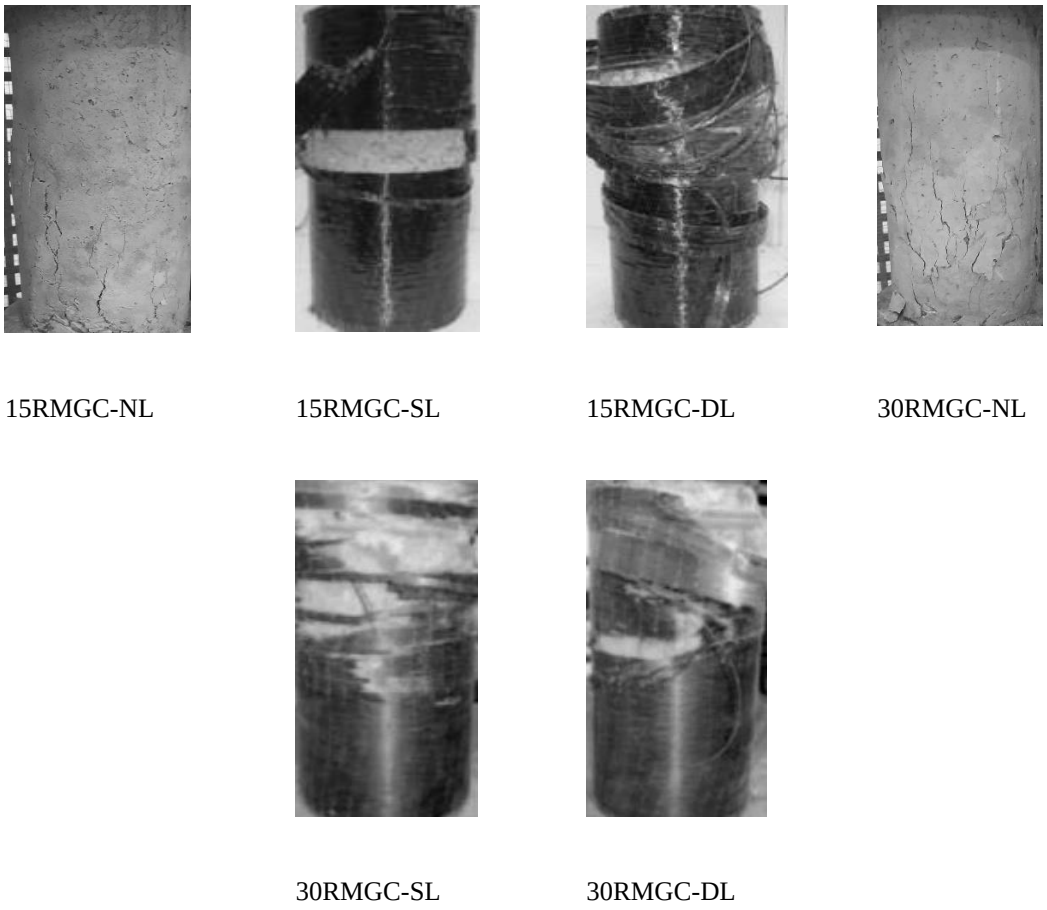

Figure 5. Failure modes and damage patterns of CFRP-confined specimens

ii. Compressive Strength

The compressive stress and axial strain results from the experimental tests are illustrated in Figure 6. It was observed that the number of CFRP layers significantly influenced the compressive stiffness of the cylinders. Typically, the compressive stiffness of the confined concrete increased with the addition of CFRP layers, from one to two. This enhancement in stiffness is attributed to the added confinement provided by the additional CFRP layers, which limited the lateral expansion of the concrete under compression and produced a more rigid response [9, 10]. The impact of various CFRP layer configurations on the compressive stiffness and stress-strain behavior of concrete cylinders was assessed experimentally, yielding valuable insights for the design and enhancement of CFRP-confined concrete structures.

The testing involved 36 cylindrical samples with target strengths of 15 MPa and 30 MPa. This resulted in variations in compressive strength and axial strain of 9.83% and 9.30%, respectively. For samples with a single CFRP layer, the average compressive strength of the 15 MPa specimens was recorded at 32.65 MPa, with strain values of 0.0056 and 0.0059. The corresponding discrepancies in axial strain and compressive strength were 13.05% and 5.36%, respectively. In comparison, the double-layer (DL) specimens with a target strength of 15 MPa achieved an average compressive strength of 38.23 MPa, with differences of 8.95% and 8.96% in compressive strength and axial strain, respectively. For single-layer (SL) specimens with a target strength of 30 MPa, the compressive strength was 45.70 MPa, with strain values of 0.0049.

Further analysis revealed that for specimens with a compressive strength of 15 MPa, SL and DL configurations increased the average compressive strength by 91.77% and 153.85%, respectively. Similarly, specimens with a target strength of 30 MPa showed increases in compressive strength of 52.28% and 99.33%, respectively. The CFRP confinement resulted in better performance for the 15 MPa specimens

compared to the 30 MPa specimens, indicating that lower-strength samples benefit more from the FRP confinement mechanism. For the 15 MPa specimens, SL and DL designs improved axial strain by 30.23% and 55.81%, respectively, following a similar trend to the improvements in compressive strength. The 30 MPa samples exhibited improvements in axial strain of 25.64% and 51.28%, respectively.

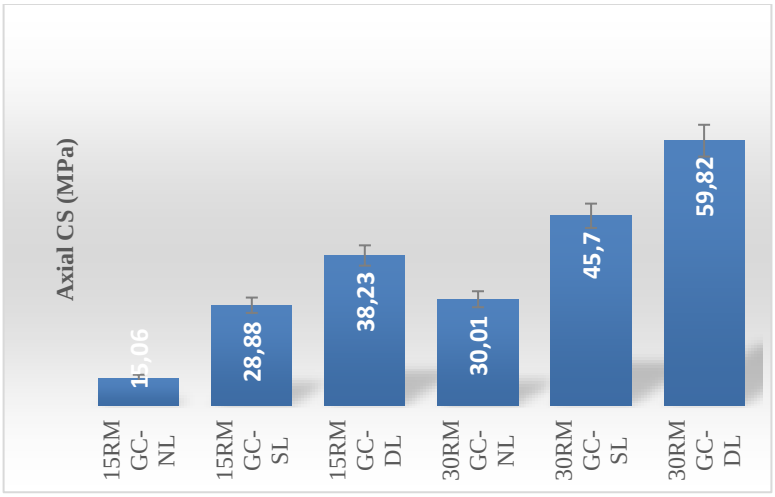

(a)

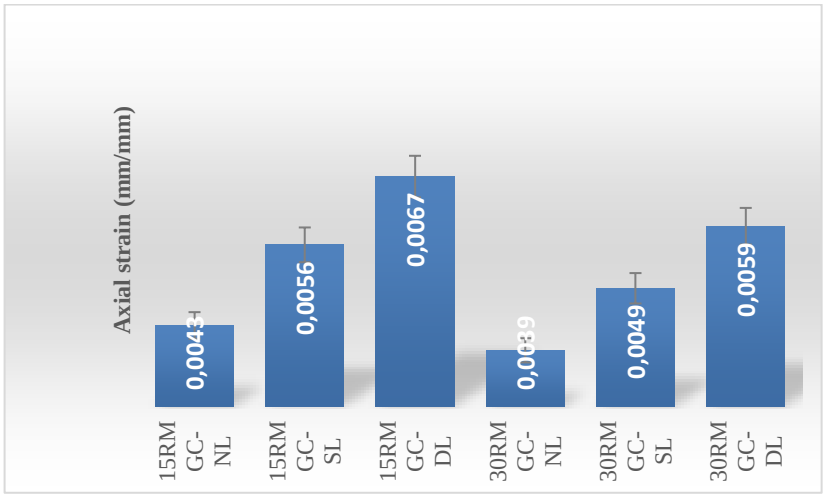

(b)

Figure 6. Axial compressive strength and axial strain at peak compressive strength.

Figure 7 illustrates the stress-strain curves under pure axial compression for each group of samples. The data reveal that the ductility and strength of RMGC samples were significantly enhanced by the confining effect provided by FRP. Analysis indicates that the strength improvement correlates with the extent of confinement, which depends on the number of FRP layers. Specifically, specimens with lower strength (15 MPa) experienced a greater impact from the confining effect compared to those with higher strength (30 MPa). Consequently, for RMGC specimens with lower strength, the confining effect was more beneficial for both axial compressive strength and strain. Figure 7 also presents the complete stress-strain behaviour for test samples with strengths of 15 MPa and 30 MPa across all groups. The FRP-based confinement method substantially increased the axial stiffness of low-strength specimens. The axial compressive strength of RMGC samples subjected to 15 MPa and 30 MPa improved with the addition of more FRP layers. The study found that for 15 MPa samples, those with the SL configuration exhibited higher compressive strength compared to those with the DL structure. Additionally, for 30 MPa samples,

increasing the number of FRP layers significantly enhanced compressive strength, demonstrating that additional FRP layers greatly boost the compressive strength of high-strength concrete. The stress-strain data also indicated that low-strength RMGC samples showed a marked improvement in ductility with more FRP layers. The stress-strain curves in Figure 7 illustrate the trend of increased axial deformation and strength enhancement.

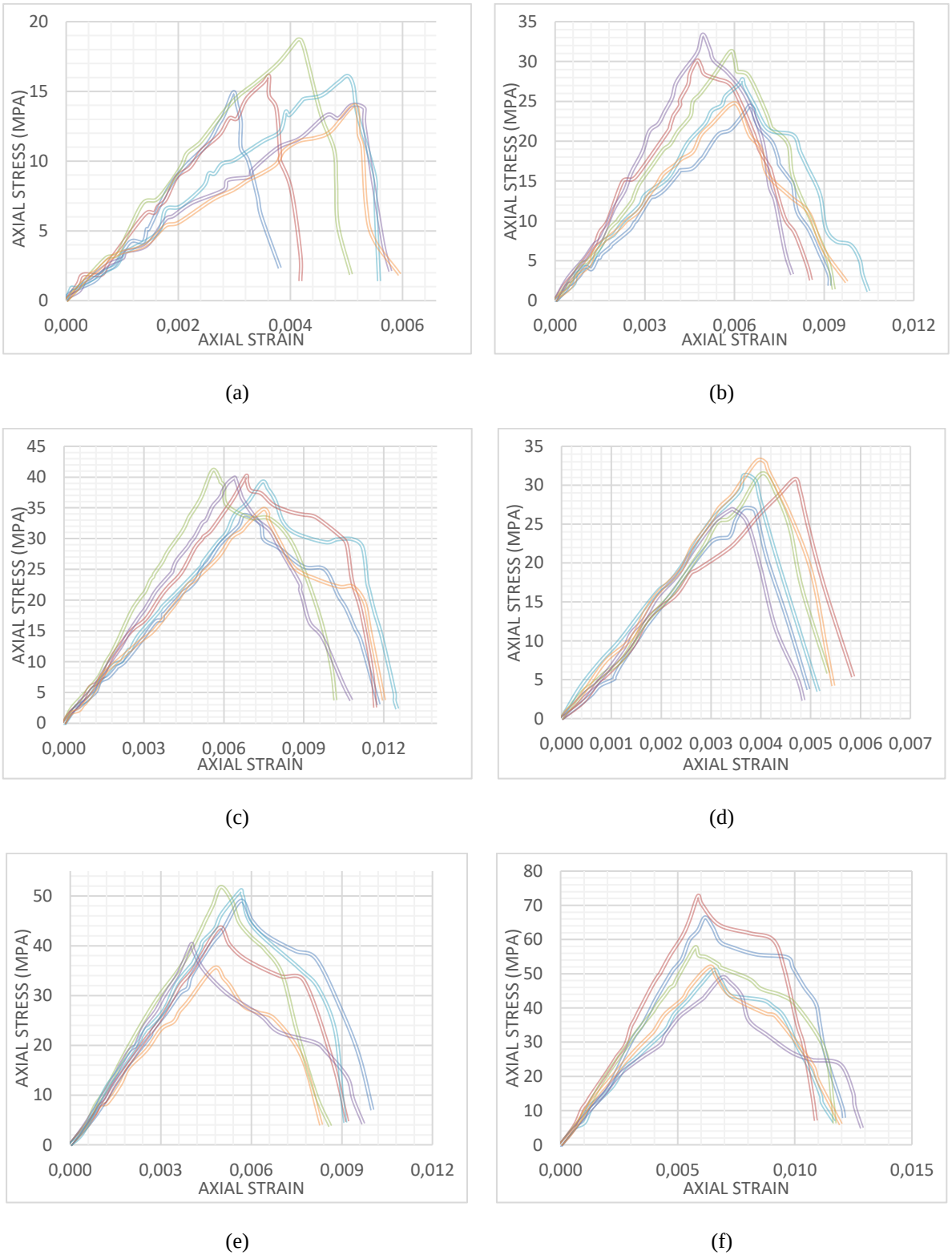

Figure 7. Complete stress-strain plots for samples with a compressive strength of (a) 15RMGC-NL (b) 15RMGC-SL (c) 15RMGC-DL (d) 30RMGC-NL (e) 30RMGC-SL (f) 30RMGC-DL

IV. CONCLUSION

The following deductions were made:

- FRP-confined RMGC specimens showed similar behaviours, with fiber composites enhancing both strength and strain. For 15 MPa samples, single-layer (SL) confinement increased strength to 28.88 MPa, while double-layer (DL) confinement reached 38.23 MPa. For 30 MPa samples, SL and DL configurations resulted in strengths of 45.70 MPa and 59.82 MPa, respectively.
- Ductility and Strength Enhancement: FRP confinement significantly improved ductility and strength. For 15 MPa samples, strength increased by up to 153.85% with DL confinement, and for 30 MPa samples, up to 99.33%. Peak axial strain improvements were also notable.
- Effectiveness of FRP Confinement: FRP confinement was more effective for lower strength RMGC samples, with less pronounced benefits for 30 MPa samples compared to 15 MPa samples.

REFERENCES

[1] Ye, N., et al., Transformations of Na, Al, Si and Fe species in red mud during synthesis of one-part geopolymers. Cement and concrete research, 2017. 101: p. 123-130.

[2] Hu, Y., et al., Role of Fe species in geopolymer synthesized from alkali-thermal pretreated Fe-rich Bayer red mud. Construction and Building Materials, 2019. 200: p. 398-407.

[3] Han, Y.-S., et al., Bauxite residue neutralization with simultaneous mineral carbonation using atmospheric CO2. Journal of Hazardous Materials, 2017. 326: p. 87-93.

[4] Santillán, L., et al., Long-term sulfate attack on recycled aggregate concrete immersed in sodium sulfate solution for 10 years. Materiales de Construcción, 2020. 70(337): p. 212.

[5] Raza, A., et al., Finite element modelling and theoretical predictions of FRP-reinforced concrete columns confined with various FRP-tubes. Structures, 2020. 26: p. 626-638.

[6] Raza, A., et al., Strength Profile Pattern of FRP-Reinforced Concrete Structures: A Performance Analysis through Finite Element Analysis and Empirical Modeling Technique. Polymers, 2021. 13(8): p. 1265.

[7] Raza, A. and Q.u.Z. Khan, Efficiency of GFRP reinforcement in concrete columns having hybrid fibres: experiments and finite element analysis. Magazine of Concrete Research, 2022. 74(21): p. 1103-1119.

[8] Raza, A., M.H. El Ouni, and M. Berradia, Structural Assessment of Eccentrically Loaded GFRP Reinforced Circular Concrete Columns: Experiments and Finite Element Analysis. Composite Structures, 2021: p. 114528.

[9] Raza, A., Q.u.Z. Khan, and A. Ahmad, Prediction of axial compressive strength for FRP-confined concrete compression members. KSCE Journal of Civil Engineering, 2020. 24(7): p. 2099-2109.

[10] Raza, A., et al., Effectiveness of FRP confinement for low strength recycled aggregate concrete compressive members having optimized combination of fibers. Structural Concrete, 2024. 25(2): p. 1092-1104.